Proceedings of the Seventh International Conference on Research in Intelligent and Computing in Engineering pp. 195–200 DOI: 10.15439/2022R33 ISSN 2300-5963 ACSIS, Vol. 33

Decoupling Sliding Mode Control of Underactuated Systems using a Takagi-Kang-Sugeno Fuzzy Brain Emotional Controller and Particle Swarm Optimization

Duc-Hung Pham
Faculty Electrical and Electronic Engineering, Hung Yen University of Technology and Education, Hai Duong, Vietnam.
phamduchunghp@gmail.com

Viet- Ngu Nguyen
Faculty Electrical and Electronic Engineering, Hung Yen University of Technology and Education, Hung Yen, Vietnam.
Ngunguyenviet77@gmail.com

Thi Minh- Tam Le
Faculty Electrical and Electronic Engineering, Hung Yen University of Technology and Education, Hung Yen, Vietnam
leminhtamutehy@gmail.com

***Abstract*—A Tagaki-Kang-Sugeno fuzzy brain emotional controller (TFBEC) for decoupling control of underactuated nonlinear systems is developed in this paper. The decoupling sliding mode technique is used to achieve decoupling control performance. An amygdala cortex and a prefrontal cortex comprise the brain emotional model. The prefrontal cortex is an emotional neural network, while the amygdala cortex is a sensory neural network. The proposed TFBEC is adaptive, and the parameters can be adjusted to achieve efficient control performance. A TFBEC is used as the main controller to approximate an ideal controller and achieve the desired control performance, and a robust compensator is used to eliminate the remaining approximation error and achieve system stability. A particle swarm optimization is used to find the optimal learning rates of the proposed method. Finally, the TFBEC control system is demonstrated by controlling a bridge crane system with one degree of under actuation. Simulation results have confirmed the validity of the proposed approach.**

***Keywords*—Takagi-Kang-Sugeno fuzzy system, brain emotional controller, bridge-crane system.**

I. INTRODUCTION

For a specific type of underactuated nonlinear systems, the decoupling sliding mode control (DSMC) was developed. Separated into their own second-order systems, all subsystems need both a primary and secondary control function. Discrete subsystems' state variables can be thought of as sliding surfaces. For these sliding surfaces, we develop a primary goal condition and a secondary goal condition, with an intermediate variable taken from the sub-sliding surface condition to account for these subsystems [1]. The concept of sliding mode control (SMC) has recently been introduced as a means of controlling nonlinear systems whose dynamics are unknown.

LeDoux [3] initially observed in 1992 that emotions are critical to human perception and action. In 2001, Balkenius and Moren [4] created a model of emotional learning in the brain that was grounded in neurophysiology. To this end, they developed and tested in virtual reality a brain with a synthetic amygdala and frontal lobe. The creation of a model of emotional learning has received a lot of attention in recent years. The Brain Emotional Learning Controller (BELC), introduced by Lucas et al [5], is a notable example of a system built using this paradigm. The amygdala cortex and the sensory network in this BELC are in constant dialogue with one another, just as the orbitofrontal cortex and its counterpart do in the human brain. The BELC performs well in dynamic systems because of its rapid self-learning capability, low implementation complexity, and great robustness.

Decoupled sliding mode control (DSMC) alone is not enough to make highly nonlinear objects easier to control. Recent research that combines DSMC with neural networks, like the fuzzy neural network [6], has produced impressive results. Based on this direction of growth, this study suggests combining DSMC with a new controller called Takagi-Kang-Sugeno fuzzy brain emotional controller (TFBEC).

There are two kinds of fuzzy systems: 1) Takagi-Sugeno-Kang (TSK) fuzzy systems and 2) Mamdani fuzzy systems [7]. In TSK fuzzy systems, the "IF" parts of the TSK rules match the "IF" parts of other fuzzy inference rules. In general, the "THEN" part of TSK rules is a polynomial function of the input variables. This BELC has a new fuzzy neural network called TSK Fuzzy Brain Emotional Controller (TFBEC), which uses the TSK fuzzy inference algorithm. Both the TSK fuzzy neural network and the BELC have advantages that the TFBEC also has. The parameter update laws of the TFBEC are worked out, and a Lyapunov function is used to show that the control system is stable. A second controller is needed to act like the ideal controller. The auxiliary controller might be a good one [8].

The remainder of this paper can be summarized as follows: Section II discusses the problem formulation, Section III discusses the proposed TFBEC and the PSO method, Section IV discusses the simulation results, and Section V concludes the paper.

II. PROBLEM FORMULATION

Consider a nonlinear system with underactuated expressed in the following form [1]

$$\begin{cases} \dot{y}_1 = y_2 \\ \dot{y}_2 = g_1(y_1, y_2) + b_1(y_1, y_2)u + d_1 \\ \dot{y}_3 = y_4 \\ \dot{y}_4 = g_2(y_1, y_2) + b_2(y_1, y_2)u + d_2 \end{cases} \quad (1)$$

where $g_1(y_1, y_2)$, $g_2(y_1, y_2)$ and $b_1(y_1, y_2)$, $b_2(y_1, y_2)$ are bounded nominal nonlinear functions, $\boldsymbol{y} = [y_1 \; y_2 \; y_3 \; y_4]^T \in \Re^4$ is the state vector, u is the control input; and d_1 and d_2 are the external disturbances. This system can be viewed as two subsystems, each with a second-order canonical two subsystems with second-order canonical form that includes the corresponding states (y_1, y_2) and (y_3, y_4). The decoupling control seeks to develop a single input u that simultaneously controls the states (y_1, y_2) and (y_3, y_4) to achieve the desired performance. The tracking error is defined as follows:

$$\begin{cases} e_1 = y_{d1} - y_1 \\ e_2 = y_{d2} - y_2 \\ e_3 = y_{d3} - y_3 \\ e_4 = y_{d4} - y_4 \end{cases} \quad (2)$$

where $\boldsymbol{y}_d = [y_{1d} \;\; y_{2d} \;\; y_{3d} \;\; y_{4d}]^T \in \Re^4$ is the reference trajectory. Defining the coupling sliding surface for this system as [8]

$$s = \xi_1(e_1 - \omega) + e_2 \quad (3)$$

$$z = \xi_2 e_3 + e_4 \quad (4)$$

where ξ_1, ξ_2 selected coefficients correspond to those of a Hurwitz polynomial, and ω is derived from z and is defined as

$$\omega = \text{sat}(z / \Phi_\omega)\omega_u, \quad 0 < \omega_u < 1 \quad (5)$$

where Φ_ω is the boundary layer of z. Φ_ω transfers z to the correct range of y_1, and the definition of sat(.) function is:

$$\text{sat}(z / \Phi_\omega) = \begin{cases} \text{sgn}(z / \Phi_\omega), & \text{if } |z / \Phi_\omega| \geq 1 \\ z / \Phi_\omega, & \text{if } |z / \Phi_\omega| < 1 \end{cases} \quad (6)$$

where $\omega_u \leq 1$ therefore ω is a decaying oscillation signal

From (1), an ideal controller u_{ideal} can be represented as

$$u_{ideal} = b_1^{-1}\left(-\xi_1 y_2 - \xi_1 \dot{\omega} - g_1 + \xi_1 \dot{y}_{1d} + \dot{y}_{2d} - d_1\right) \quad (7)$$

u_{ideal} in (7) is unavailable due to an unidentified problem. Thus, a TFBEC is presented as a controller that approaches perfection.

III. TAKAGI-KANG-SUGENO FUZZY BRAIN EMOTIONAL CONTROLLER

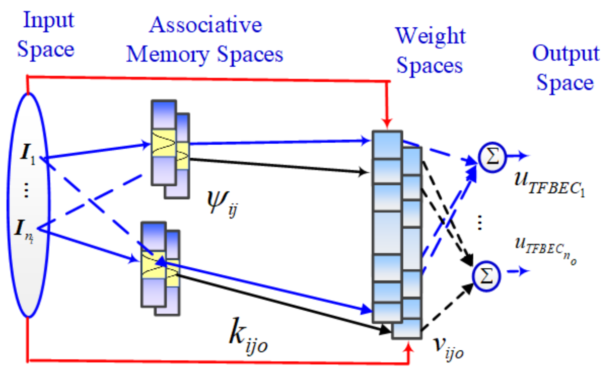

Fig. 1. The structure of TFBEC

The suggested TFBEC is depicted in Figure 1. The TFBEC employs the TSK fuzzy inference rules:

If I_1 is f_{1jo}, I_2 is f_{2jo}, …, and I_{n_i} is $f_{n_i jo}$

then $u_o = I_1 k_{1jo} + I_2 k_{2jo} + \ldots + I_{n_i} k_{n_i jo}$ (8)

for $o = 1, 2, \ldots, n_o$; $j = 1, 2, \ldots, n_j$

(8)

where I_i is the input of the fuzzy inference system; k_{ijo} and u_o are respectively the TSK weight and the TFBEC output. Signal propagation and fundamental function in each TFBEC space are described as follows:

A. Input Space

For the input data, $I = [I_1, I_2, \ldots, I_{n_i}] \in \Re^{n_i}$, n_i is the input dimension.

B. Association Memory Space

In Sensory cortex space, the sigmoid function is adopted represented as:

$$\psi_{ij} = \exp\left(-\left(\frac{I_i - m_{ij}^B}{\sigma_{ij}^B}\right)^2\right) \quad (9)$$

where ψ_{ij} is the Gaussian function of prefrontal system input and amygdala system input for sensory cortex output, m_{ij}^B and σ_{ij}^B are respectively mean and variance.

C. Emotional Weight Space

This space uses the inference fuzzy rules as follows:

If I_1 is ψ_{1j}, I_2 is ψ_{2j}, …., and I_{n_i} is $\psi_{n_i j}$ then

$$v_{jo} = \sum_{i=1}^{n_i} (I_i k_{ijo}) \quad (10)$$

for $o = 1, \ldots, n_o$; $j = 1, \ldots, n_j$; $i = 1, \ldots, n_i$

D. Output Space

The output space is represented as follows

$$u_{TFBEC_o} = \sum_{i=1}^{n_i}\sum_{j=1}^{n_j}\psi_{ij}v_{jo} = \sum_{i=1}^{n_i}\sum_{j=1}^{n_j}\psi_{ij}\sum_{i=1}^{n_i}(I_i k_{ijo}) \quad (11)$$

for $o = 1,\ 2, \dots,\ n_o$

A cost function is defined as $V_1 = \frac{1}{2}s^2$, then the derivate of it is $\dot{V}_1 = s\dot{s}$. Using the gradient descent method to find the proposed method's updating laws. The following equations describes the updated laws.

$$k_{ijo}(t+1) = k_{ijo}(t) + \Delta k_{ijo} \quad (12)$$

$$m_{ij}^B(t+1) = m_{ij}^B(t) + \Delta m_{ij}^B \quad (13)$$

$$\sigma_{ij}^B(t+1) = \sigma_{ij}^B(t) + \Delta\sigma_{ij}^B \quad (14)$$

$$\Delta k_{ijo} = -\lambda_k.\frac{\partial \dot{V}_1}{\partial k_{ijo}} = -\lambda_k.\frac{\partial(s\dot{s})}{\partial k_{ijo}} = -\lambda_k.\frac{\partial(s\dot{s})}{\partial u_{TFBEC_o}}.\frac{\partial u_{TFBEC_o}}{\partial k_{ijo}} = -\lambda_k.b_1.s.\psi_{ij}\sum_{i=1}^{n_i} I_i \quad (15)$$

$$\Delta m_{ij}^B = -\lambda_m.\frac{\partial \dot{V}_1}{\partial m_{ij}^B} = -\lambda_m.\frac{\partial(s\dot{s})}{\partial m_{ij}^B} = -\lambda_m.\frac{\partial(s\dot{s})}{\partial u_{TFBEC_o}}.\frac{\partial u_{TFBEC_o}}{\partial \psi_{ij}}.\frac{\partial \psi_{ij}}{\partial m_{ij}^B} = -\lambda_m b_1 s\sum_{i=1}^{n_i}(I_i k_{ijo}).\ \frac{2(I_i - m_{ij}^B)}{(\sigma_{ij}^B)^2} \quad (16)$$

$$\Delta\sigma_{ij}^B = -\lambda_\sigma.\frac{\partial \dot{V}_1}{\partial \sigma_{ij}^B} = -\lambda_\sigma.\frac{\partial(s\dot{s})}{\partial \sigma_{ij}^B} = -\lambda_\sigma.\frac{\partial(s\dot{s})}{\partial u_{TFBEC_o}}.\frac{\partial u_{TFBEC_o}}{\partial \psi_{ij}}.\frac{\partial \psi_{ij}}{\partial \sigma_{ij}^B} = -\lambda_\sigma.b_1.s\sum_{i=1}^{n_i}(I_i k_{ijo}).\frac{2(I_i - m_{ij}^B)^2}{(\sigma_{ij}^B)^3} \quad (17)$$

where λ_k, λ_m, and λ_σ are learning rates with positive values. The learning rates can be optimized by the PSO algorithm. The approach error causes a tracking error in the control system because the TFBEC cannot perfectly replicate the ideal controller. As a result, a compensating controller is required to ensure the control system's robust stability. The control system is depicted in Figure 2.

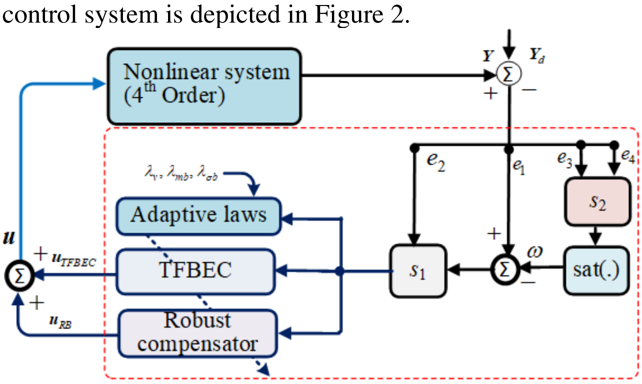

Fig. 2. Block diagram of TFBEC control system

When we take the derivative of (3), we get the following:

$$\dot{s} = \xi_1(\dot{e}_1 - \dot{\omega}) + \dot{e}_2 = \xi_1\left(\dot{y}_{1d} - \dot{y}_1 - \dot{\omega}\right) + \dot{y}_{2d} - \dot{y}_2 \quad (18)$$

Due to the inevitability of an approximation error between the TFBEC and the ideal controller, the latter can be expressed as the sum of the former and the latter, with the assumption that the approximation error is defined as

$$\Delta = u_{ideal} - u_{TFBEC} \quad (19)$$

The control system is structured as follows to account for the approximation error:

$$u = u_{TFBEC} + u_{RB} \quad (20)$$

$$u_{RB} = \hat{\mu}\,\text{sign}(s) \quad (21)$$

where $\hat{\mu}$ is an estimated value of the variable μ being looked up. Then the adaptive law of $\hat{\mu}$ is as follows.

$$\dot{\hat{\mu}} = \lambda_\mu |s| \quad (22)$$

Picking a Lyapunov function using the formula

$$V = \frac{1}{2}s^2 + \frac{\tilde{\mu}\tilde{\mu}}{2\lambda_\mu} \quad (23)$$

Then, the derivate of V is attained

$$\dot{V} = s(\sigma - u_{RB}) + \frac{\tilde{\mu}\dot{\tilde{\mu}}}{\lambda_\mu} = s\left(\sigma - \hat{\mu}\,\text{sign}(s)\right) + \frac{\tilde{\mu}\dot{\tilde{\mu}}}{\lambda_\mu} = s\sigma - \hat{\mu}|s| + \frac{\tilde{\mu}\dot{\tilde{\mu}}}{\lambda_\mu} \quad (24)$$

Because $\mu = \tilde{\mu} + \hat{\mu}$ is constant so: $\dot{\tilde{\mu}} = -\dot{\hat{\mu}} = -\lambda_\mu |s|$ therefore

$$\dot{V} = s\sigma - \hat{\mu}|s| - (\mu - \hat{\mu})|s| = -(\mu - |\sigma|)|s| \le 0 \quad (25)$$

Since $\dot{V} \le 0$, $V \le V(0)$, provides that $\tilde{\mu}$ and s are bounded. Defining $\Lambda = (\mu - |\sigma|)s \le (\mu - |\sigma|)|s| \le -\dot{V}$. Integrating Λ with respect to time, obtains:

$$\int_0^t \Lambda(\tau)d\tau \le V(0) - V(t) \quad (26)$$

Since $V(0)$ and $\dot{V}(t)$ are both constrained, $\dot{V}(t)$ is not increased, so $\lim_{t\to\infty}\int_0^t \Lambda(\tau)d\tau < \infty$. This points to the fact that $t \to \infty \Rightarrow s \to 0$. As a result, the TFBEC control method that was suggested has a high degree of guaranteed stability.

E. Particle Swarm Optimization (IPSO)

Particle swarm optimization (PSO) is an efficient optimization method recommended by Eberhart and Kennedy [12]. To obtain suitable learning rates λ_k, λ_m, and λ_σ for the update laws of TFBEC, the improved PSO algorithm is used [12]. The algorithm calculates the fitness function of each set, and then each set can be adjusted based on the local optimization position of the particles

L_{best_i} and the global optimization position of the swarm G_{best_i}. In this study, the fitness function is chosen as follows.

$$F = \frac{1}{|e| + 0.1} \tag{27}$$

$p_i(t)$, $\theta_i(t)$ are respectively the current velocity and the current velocity of the particle. The update of $p_i(t)$ and $\theta_i(t)$ are given as follows.

$$p_i(t+1) = p_i(t) + \theta_i(t+1) \tag{28}$$

$$\theta_i(t+1) = \zeta.\theta_i(t) + \kappa_1.\mu_1.\left(P_{best_i} - p_i(t)\right) + \kappa_2.\mu_2.\left(G_{best_i} - p_i(t)\right) \tag{29}$$

where ζ is inertia weight, κ_1 and κ_2 are learning factors, μ_1 and μ_2 are two random variables in the range [0,1], $0 \le \mu_1 \le 1$, $0 \le \mu_2 \le 1$. The PSO algorithm can be represented as follows.

Step 1: Initialization of the swarm, the position of the particles is chosen randomly.

Step 2: Calculate the fitness function for each particle. $Fit\left(p_i\right)$

Step 3: Comparison of the fitness function with its best fitness function.

If $F\left(p_i\right) < F\left(G_{best_i}\right)$ then $F\left(G_{best_i}\right) = F\left(p_i\right)$ and $p_i = G_{best_i}$

Step 4: Comparison of the fitness function $F\left(p_i\right)$ of each particle with the best global particle $F\left(G_{best_i}\right)$

If $F(p_i) < F\left(G_{best_i}\right)$ then $F\left(G_{best_i}\right) = F(p_i)$ and $p_i = G_{best_i}$.

Step 5: Update the position and velocity with (28) and (29).

Step 6: Go back to step 2 and repeat until convergence.

IV. Simulation Results

For the purposes of this section, consider the control problem of a two-dimensional bridge crane system, as seen in Figure 2 and formulated as follows [9].

$$M(q)\ddot{q} + C(q,\dot{q})\dot{q} + G(q) = u \tag{30}$$

where $q = \begin{bmatrix} x & \theta \end{bmatrix}^T$ and matrices and vectors are expressly defined as follows.

$$M(q) = \begin{bmatrix} m_x + m & ml \times \cos\theta \\ ml \times \cos\theta & ml^2 \end{bmatrix},$$

$$C(q,\dot{q}) = \begin{bmatrix} 0 & -ml \times \sin\theta \times \dot{\theta} \\ 0 & 0 \end{bmatrix},$$

$G(q) = \begin{bmatrix} 0 & mgl \times \sin\theta \end{bmatrix}^T$, $u = \begin{bmatrix} F - f_{rx} & d \end{bmatrix}^T$. Table I provides a place to define the various parameters of the system.

TABLE I
THE PAREMTERS OF BRIDGE CRANE SYSTEM

Parameter	Definiton
m_x	cart mass
m	load mass
l	cable length
x	cart displacement
θ	load swing angle
F	control input
f_{rx}	non-linear friction between the cart and the bridge
d	external disturbance
f_{r0x}, ε	static friction coefficients
k_{rx}	viscous friction

$$f_{rx} = f_{r0x} \tanh(\dot{x}/\varepsilon) - k_{rx}|\dot{x}|\dot{x} \tag{31}$$

k_{rx} can be determined through offline experimental testing and data collection. Consider the control problem in terms of putting the load at the appropriate location by simultaneously managing the horizontal motion of the carriage and minimizing the load's wobble. Specifically, we wish to push the position of the carriage x to the required place $p_d \in \Re$ while eliminating θ, which can be specified mathematically as.

$$\lim_{t\to\infty} x(t) = p_d, \qquad \lim_{t\to\infty} \theta(t) = 0 \tag{32}$$

Define $y_1 = \theta(t),\ y_2 = \dot{\theta}(t),\ y_3 = x(t),\ y_4 = \dot{x}(t)$.

From (3)-(5), the following specifications, we select $\xi_1 = 5$, $\xi_2 = 0.5$, $\Phi_\omega = 5$, $\omega_u = 0.95$. The initial values are as follows: $m_x = 7\ [kg]$, $m = 1.025\ [kg]$, $l = 4\ [m]$, $p_d = 0.6\ [m]$, $x(0) = 0$, $\theta(0) = 0$. To test the effect of control effort in the presence of external disturbances, add wind speed as a disturbance during transport to validate at t=7 [s] $d = -45$ [N], at t=8 [s] $d = 45$ [N], at t=9 [s] $d = -55$ [N], and at t=10 [s] $d = 55$ [N]. The initial values for TFBEC are:

n_i=2, n_j=8, n_k=2, n_o=2,

$m_{11}^B = m_{21}^B = -1, m_{12}^B = m_{22}^B = -0.75, m_{13}^B = m_{23}^B = -0.5,$
$m_{14}^B = m_{24}^B = -0.25, m_{15}^B = m_{25}^B = 0, m_{16}^B = m_{26}^B = 0.25,$
$m_{17}^B = m_{27}^B = 0.5, m_{18}^B = m_{28}^B = 0.75$;
$\sigma_{11}^B = \sigma_{21}^B = -0.8, \sigma_{12}^B = \sigma_{22}^B = -0.6, \sigma_{13}^B = \sigma_{23}^B = -0.4,$
$\sigma_{14}^B = \sigma_{24}^B = -0.2, \sigma_{15}^B = \sigma_{25}^B = 0, \sigma_{16}^B = \sigma_{26}^B = 0.2,$
$\sigma_{17}^B = \sigma_{27}^B = 0.4, \sigma_{18}^B = \sigma_{28}^B = 0.6$; λ_k=0.05, $\lambda_m = 0.05$, and λ_σ =0.01. The initial value of PSO: ζ=0.9 , $\kappa_1 = \kappa_2 = 0.02$, $\mu_1 = \mu_2 = 0.001$, and $\theta_i = 0.002$.

The results of the simulation are presented in Figures 4-7, and Table II has a listing of the Root Mean Square Error (RMSE). The root mean square error (RMSE) of the sliding mode control (SMC) [10] and the FBELC [11] is smaller than the RMSE of the proposed TFBEC for θ (RMSE_ θ), which is 2.48 times and 1.01 times smaller, respectively. And the root mean square error of the suggested TFBEC for X, which is denoted by RMSE X, is 1.67 times smaller than the RMSE of

SMC and 1.17 times smaller than the RMSE of FBELC, respectively. However, because of the complexity of TFBEC, the amount of time needed to complete computations using our method is significantly longer. The process of changing the learning rates λ_k, λ_m, and λ_σ using the PSO algorithm is depicted in Figure 4. This demonstrates that the PSO algorithm is effective since after the first fluctuation in the learning rate values, those values eventually settle down to a constant positive value. Figure 5 demonstrates that the output of is less volatile when utilizing the proposed TFBEC in comparison to the output of conventional controllers, and that this leads to a more rapid transition to steady state. The results of X that are displayed in Fig. 6 are comparable to those displayed in Fig. 5. Figure 7 illustrates how the control efforts are altered when an external disturbance is present. The suggested TFBEC is able to adjust to noise more quickly than the SMC and the FBELC.

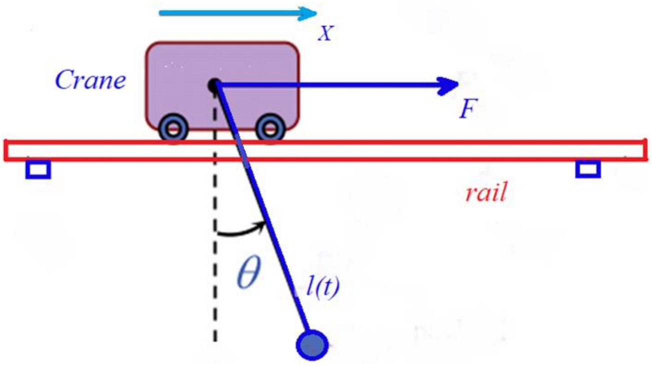

Fig. 3. A 2-dimensional underactuated bridge-crane

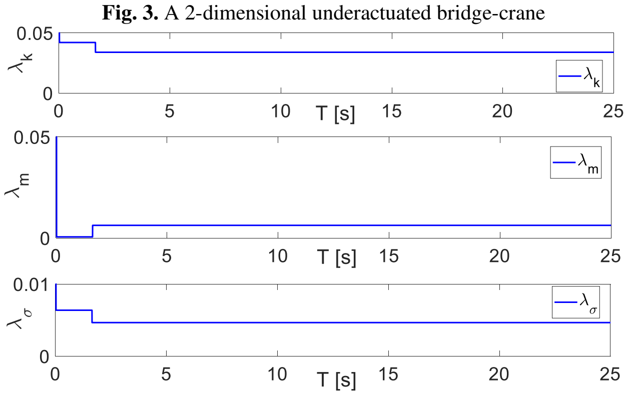

Fig. 4. The updating of learning rates using PSO algorithm.

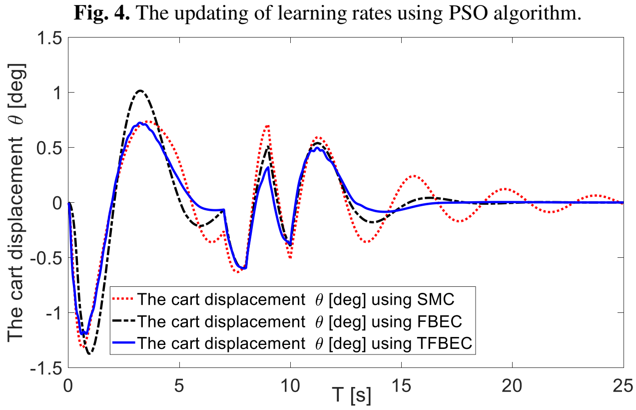

Fig. 5. The control results for the bridge crane for θ

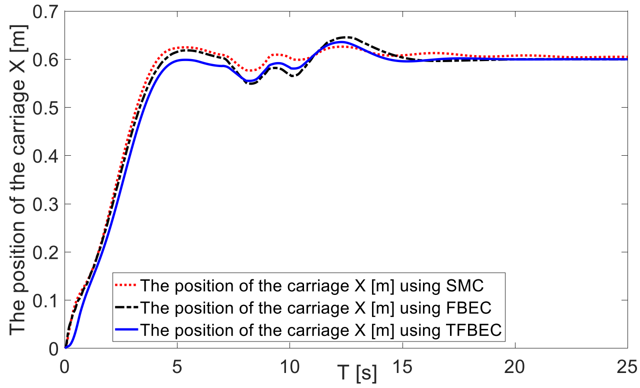

Fig. 6. The control results for the bridge cranes for X

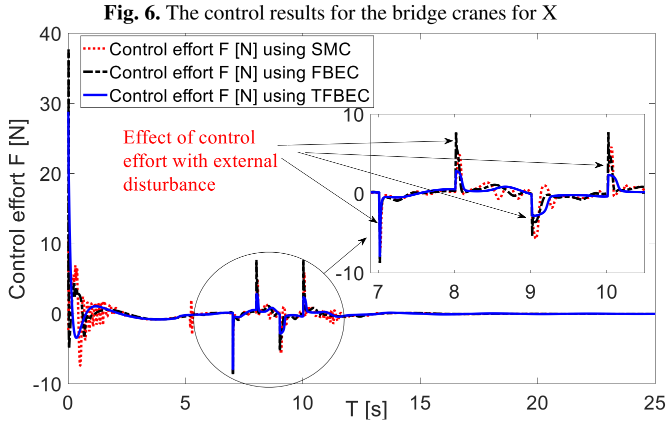

Fig. 7. The control effort F [N] for the bridge cranes

TABLE II
COMPARISION IN RMSE FOR BRIDGE CRANE SYSTEM

Method	Computation time [s]	RMSE_θ	RMSE_X
SMC [10]	0.085	0.380	0.01
FBELC [11]	0.175	0.155	0.007
The proposed TFBEC	0.234	0.153	0.006

V. CONCLUSION

It has been suggested that TFBEC can be used to decouple the control of nonlinear systems. In addition, the optimum values of the learning rates can be determined by the use of PSO. The results of a simulation run on a nonlinear bridge crane are shown, demonstrating that the effectiveness of the suggested control system was confirmed by the simulation. The developed controller is successful in properly tracking the target while making only minor errors and demonstrates rapid convergence.

REFERENCES

[1] F. Yorgancioglu, and H. Komurcugil, "Decoupled sliding-mode controller based on time-varying sliding surfaces for fourth-order systems," *Expert Systems with Applications*, vol. 37, no. 10,pp. 6764-6774, 2010.

[2] K. J. Å ström and B. Wittenmark, Adaptive Control, Reading, *Addision-Wesly,* Massachusetts, 1995.

[3] J. E. LeDoux, The Amygdala: Neurobiological Aspects of Emotion, *Wiley-Liss, New York*, pp. 339-351, 1992.

[4] C. Balkenius and J. Moren, "Emotional learning: A computational model of the amygdala," *Cybernetics and Systems*, vol. 32, no. 6, pp. 611-636, 2001.

[5] C. Lucas, D. Shahmirzadi, and N. Sheikholeslami, "Introducing BELBIC: Brain emotional learning based intelligent controller,"

International Journal of Intelligent Automation and Soft Computing, vol. 10, no. 1, pp. 11-21, 2004.

[6] L.–C. Hung and H.-Y. Chung, “Decoupled sliding-mode with fuzzy-neural network controller for nonlinear systems,” *International Journal of Approximate Reasoning*,vol. 46, no. 1, pp 74-97, 2007.

[7] Lin, C. M., Pham, D. H., & Huynh, T. T. “Encryption and Decryption of Audio Signal and Image Secure Communications Using Chaotic System Synchronization Control by TSK Fuzzy Brain Emotional Learning Controllers,” *IEEE Transactions on Cybernetics*, 2021, . doi: 10.1109/TCYB.2021.3134245.

[8] T.-T. Huynh, C. –M. Lin, N.-Q. –K. Le, N. P. -Nguyen, and F. Chao. "Intelligent wavelet fuzzy brain emotional controller using dual function-link network for uncertain nonlinear control systems." *Applied Intelligence*, vol. 52, no. 3, pp. 2720-2744, 2022.

[9] N. Sun, Y.-C. Fang, and X.-Q. Wu, "An enhanced coupling nonlinear control method for bridge cranes," *IET Control Theory and Applications,* vol. 8, no.13, pp. 1215-1223, 2014.

[10] C. M. Lin, and Y. J. Mon, "Decoupling control by hierarchical fuzzy sliding-mode controller," *IEEE Transactions on Control Systems Technology,* vol. 13, no. 4, pp. 593-598, 2005.

[11] C.-M. Lin, D.-H. Pham, and T.-T. Huynh, “Synchronization of chaotic system using a brain-imitated neural network controller and its applications for secure communications,” *IEEE Access,* vol. 9, pp. 75923-75944, 2021.

[12] R. Eberhart and J. Kennedy, "A new optimizer using particle swarm theory," in *MHS'95. Proceedings of the Sixth International Symposium on Micro Machine and Human Science*, 1995, pp. 39-43: IEEE.